ACS OMEGA

http://pubs.acs.org/journal/acsodf

Article

Role of 3-Methacryloxypropyltrimethoxysilane in Dentin Bonding

Xin Jin,[‖] Xiaojun Yuan,[‖] Kai Chen, Haifeng Xie, and Chen Chen*

Cite This: *ACS Omega* 2022, 7, 15892−15900

Read Online

ACCESS | Metrics & More | Article Recommendations | Supporting Information

ABSTRACT: In this study, we aimed to examine the effect of 3-methacryloxypropyltrimethoxysilane (MPS) on dentin collagen and the impact of MPS and 10-methacryloyloxydecyl dihydrogen phosphate (MDP) together and separately on resin−dentin bonding. Eight groups of primers were prepared: control group, MDP, MPS5, MPS5 + MDP, MPS10, MPS10 + MDP, MPS15, and MPS15 + MDP. The potential interaction between MPS and collagen was assessed by molecular dynamics, contact angle measurement, zeta potential measurement, and chemoanalytic characterization using X-ray photoelectron spectroscopy, Raman spectroscopy, Fourier-transform infrared (FTIR) spectroscopy, and ultraviolet−visible spectroscopy. Microtensile bond strength (μTBS) and nanoleakage were evaluated after 24 h or 12 months of water storage. In situ zymography was used to evaluate the enzyme activity at the bonded interface. According to chemoanalytic characterization and molecular dynamics, a weak interaction between MPS and collagen was observed. MPS enhanced the hydrophobicity and negative charge of the collagen surface ($P < 0.05$). Applying an MDP-containing primer increased μTBS ($P > 0.05$) and reduced fluorescence after 24 h of water storage. Water storage for 12 months decreased μTBS ($P < 0.05$) and increased nanoleakage for all groups. MPS conditioning did not change μTBS and nanoleakage after 24 h of water storage or aging. The MPS10 + MDP and MPS15 + MDP groups presented more silver nitrate and μTBS decrease than the MDP group ($P < 0.05$). These results indicated that MPS had a weak interaction with collagen that enhanced its surface negative charge and hydrophobicity without adversely affecting dentin bonding. However, compared to MDP alone, mixing MDP with MPS impaired their effectiveness and made the dentin bonding unstable.

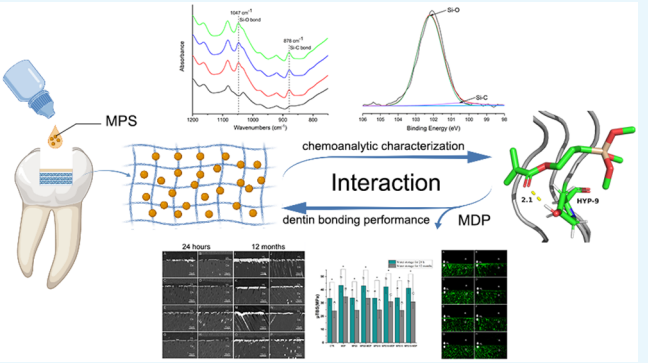

1. INTRODUCTION

Multipurpose universal adhesives that integrate multiple adhesive components for different targets in a single bottle have rapidly gained overwhelming favorability owing to their advantages of simplified clinical procedures and minimal technical sensitivity.[1] For one-bottle multipurpose universal adhesives, 3-methacryloxypropyltrimethoxysilane (MPS) is one of the most commonly employed adhesion promoters.[2] MPS has been traditionally regarded as a wetting agent, which is beneficial to hydrophobic resin penetration and achieving close contact with the hydrophilic dentin surface.[3,4] However, the more recognized function of MPS currently is to achieve chemical coupling between the acrylic resin matrix and glass-based ceramics or silicate-rich composite materials.[5−7]

Nevertheless, the functions of MPS appear to go far beyond those mentioned above and present new research possibilities. Currently available dentine bonding techniques fail to avoid the exposure of collagen fibers in the hybrid layer.[8] Moreover, the highly hydrophilic collagen fiber network is rich in water.[9] Therefore, collagen fibers without resin-matrix wrapping can trigger nanoleakage and degradation. Collagen hydrolysis in the hybrid layer is also known to negatively impact the durability of dentin adhesion and has become a significant clinical challenge.[10] Several studies have indicated that silanol is a biologically active substance and when combined with collagen fibers promotes collagen crosslinking, improving collagen stability.[11−14] The formation of activated silanols via hydrolysis is a common feature of silane compounds.[15] MPS, being a component of the adhesive, contacts the dentine surface directly during the application of the adhesive. Here, the aqueous solvent in the adhesive and residual water at the bonded interface can cause MPS to hydrolyze, generating the corresponding silanol. Therefore, one may speculate that such silanols play a role in stabilizing dentin collagen, improving the durability of dentin−resin bonding. Nevertheless, there is very little related information available in the literature with which to judge the correctness of this speculation.

Universal adhesives achieve multipurpose functionality through the use of different functional components. This

Received: February 18, 2022
Accepted: April 19, 2022
Published: April 29, 2022

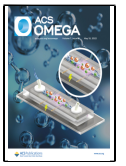

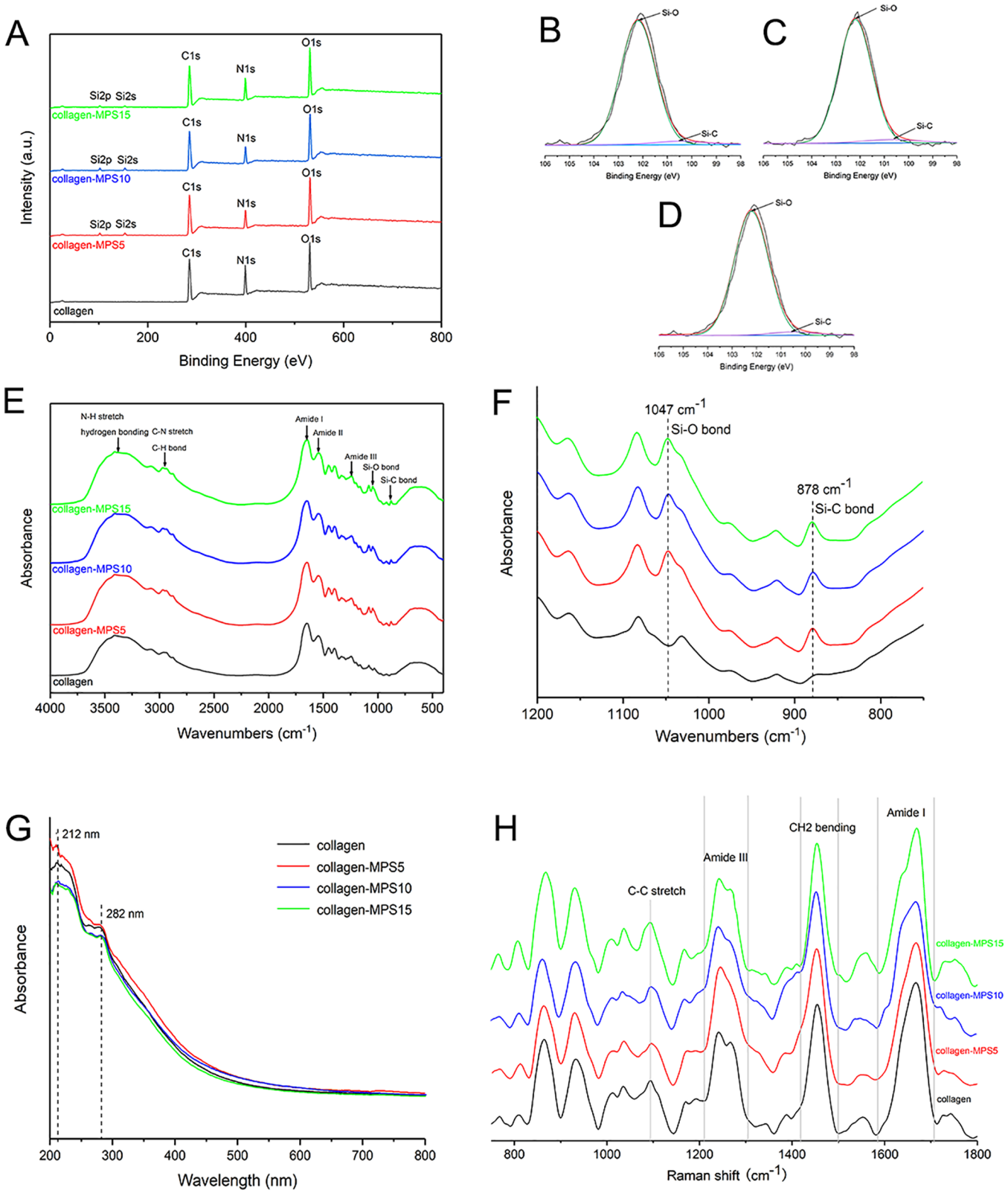

Figure 1. Wide-scan XPS spectra of the collagen powder after conditioning with MPS-containing primers (A). Si2p XPS spectra of the collagen powder conditioned with MPS5 (B), MPS10 (C), and MPS15 primer (D). FTIR spectra (E,F), UV−vis spectra (G), and Raman spectra (H) of pure collagen, collagen−MPS5, collagen−MPS10, and collagen−MPS15.

presents certain technical obstacles in terms of maintaining the relative stabilities of various ingredients when they are copresent in a single bottle. However, there is evidence that such a chemical coexistence weakens the properties of some of the functional components.[16,17]

10-Methacryloyloxydecyl dihydrogen phosphate (MDP) is another key component in universal adhesives. It plays multiple

https://doi.org/10.1021/acsomega.2c01000
ACS Omega 2022, 7, 15892−15900

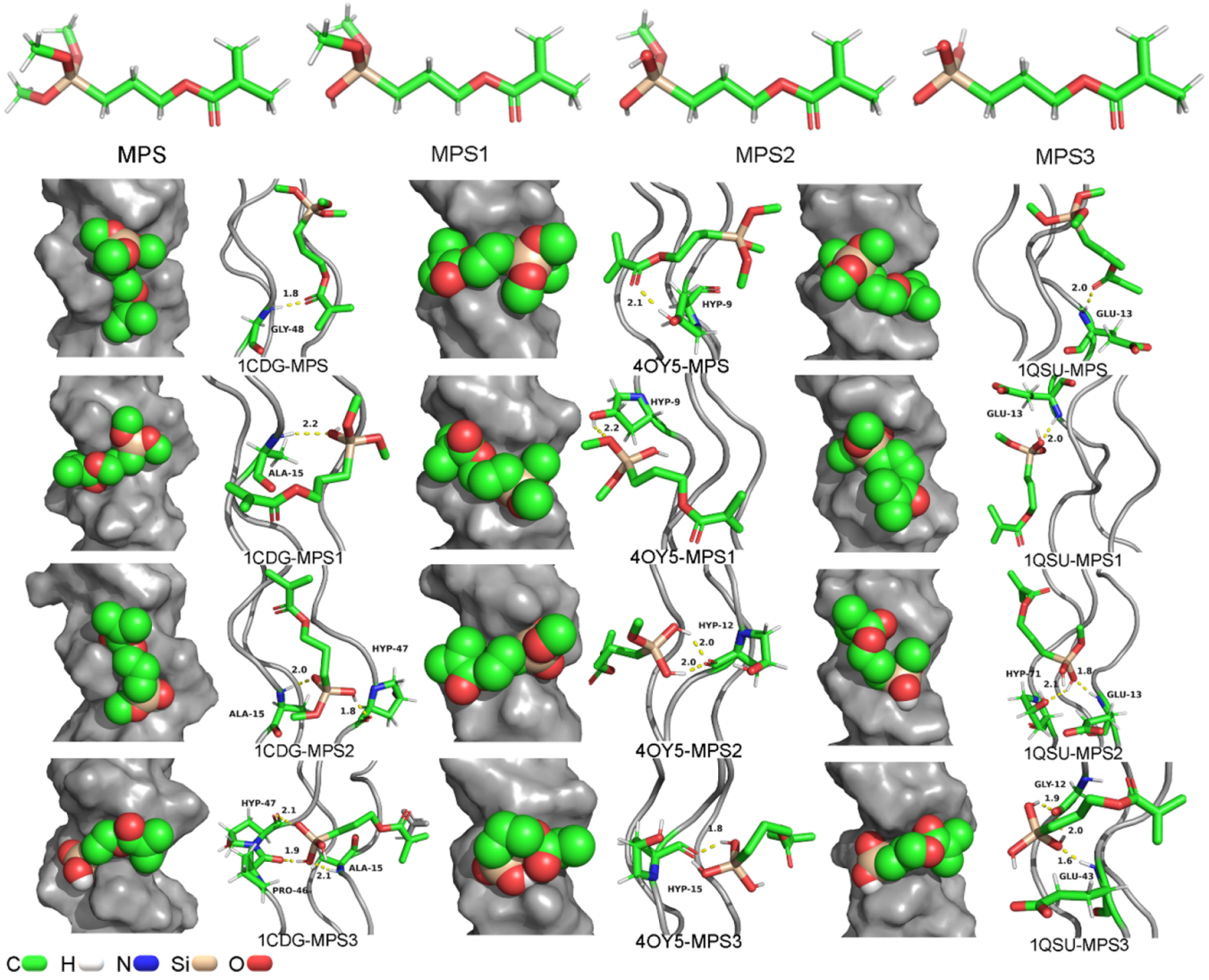

Figure 2. Representative conformations of MPS, MPS1, MPS2, and MPS3 docked on type-I collagen models (1CDG, 4OY5, and 1QSU). Hydrogen bonds are highlighted by yellow dashed lines.

roles, including demineralizing dentin,[18] forming calcium salts with hydroxyapatite,[19] improving the strength and durability of dentin−resin bonding,[20] and improving the bonding performance of metals and metal oxides such as zirconia and alumina.[21] MDP creates an acidic environment with a pH < 3, which, in turn, makes MPS prone to intramolecular self-condensation and excessive formation of inert siloxane oligomers/polymers.[22] The silanol group of MPS can undergo intermolecular condensation with the hydroxyl group of MDP to impede the positive effect of MPS on silicon-oxide-ceramic bonding.[1] Accordingly, if they are to be employed in a single-bottle formulation, the effects of chemical interference between MPS and MDP on dentin bonding durability must be carefully considered.

Accordingly, the objectives of this study were to evaluate the interaction of MPS with dentin collagen and its influence on dentin bonding and to investigate the effects of the coexistence of MPS and MDP on bonding interfaces. Multiple chemical characterization techniques and molecular dynamics simulation were used to investigate the bonding between MPS and collagen fibers. Furthermore, the potential surface-modification effects of MPS on dentine collagen and with the contribution of MPS to dentine adhesion performance (with or without MDP) were studied by contact angle and zeta potential analyses.

The following hypotheses were tested: (i) MPS binds to collagen; (ii) MPS influences the surface properties of the collagen; and (iii) the one-bottle copresence of MPS and MDP lessens their beneficial effects on resin−dentin bonding.

2. RESULTS

2.1. Interactions between Collagen and MPS. The X-ray photoelectron spectroscopy (XPS) spectra, Fourier-transform infrared (FTIR) spectra, ultraviolet−visible (UV−vis) spectra, and Raman spectra of the pure collagen, collagen−MPS5, collagen−MPS10, and collagen−MPS15 are shown in Figure 1. The major peaks in Figure 1E,H correspond to type-I collagen.[23,24] Carbon, oxygen, and nitrogen peaks can be observed in the XPS spectra of all the sample surfaces. As shown in Figure 1G, collagen has two UV−vis absorption peaks at 212 and 282 nm.[25] These results indicate that the structure of collagen is unchanged.

As shown in Figure 1A, a small amount of silicon is detected on the surface of the MPS-treated dentin. The adsorption of the MPS is confirmed by the introduction of Si 2s and Si 2p peaks at

https://doi.org/10.1021/acsomega.2c01000
ACS Omega 2022, 7, 15892−15900

102.0 and 152.5 eV. The narrow-scan Si2p spectra of MPS-treated collagen (Figure 1B−D) are consistent with Si−O and Si−C peaks at 102.3 and 100.5 eV.[26] In addition, two peaks associated with Si−C (878 cm^{-1}) and Si−O (1047 cm^{-1}) bonds are observed in all the collagen−MPS FTIR spectra in Figure 1F.[27] However, the curves for the collagen−MPS samples overlap with the control curve (Figure 1H) and there is no significant difference between them, which is due to the strong C−C stretch (1100 cm^{-1}) covering the Si−O peak.[28] Therefore, we cannot conclude that MPS has affinity for collagen.

2.2. Zeta Potential Measurement. The zeta potential results are shown in Figure S1. The silanized collagen powders show a higher negative charge compared to untreated collagen ($P < 0.001$). However, despite the increased stability of collagen with the introduction of silane, there are no significant differences in zeta potential ($P = 0.799$, 0.768, and 0.999) as the concentration of MPS increases.

2.3. Molecular Docking Simulations. MPS, MPS1, MPS2, and MPS3 were docked to form complexes with type-I collagen, revealing a potential interaction between MPS, its silanol hydrolysis product, and type-I collagen. The docking conformations of the collagen−ligand complexes are shown in Figure 2. Due to the flexibility of its molecular conformation, the ligand is embedded in a cavity orbital on the surface of the collagen molecule. Visualization of the docking sites shows that the C=O group of MPS and the silanol groups of MPS1, MPS2, and MPS3 form one or two hydrogen bonds with collagen.

The binding energies of the complexes formed by collagen 1CDG with MPS, MPS1, MPS2, and MPS3 are −2.18, −2.32, −2.60, and −2.66 kcal mol^{-1}, respectively. The binding energy between MPS and collagen 4OY5 is −0.98 kcal mol^{-1}, while the values for MPS1, MPS2, and MPS3 are −1.21, −1.46, and −1.78 kcal mol^{-1}, respectively. For collagen 1QSU, the binding energies for MPS, MPS1, MPS2, and MPS3 are −1.41, −1.55, −1.62, and −2.10 kcal mol^{-1}, respectively.

2.4. Contact Angle Measurement. Table S1 shows the water contact angle of demineralized dentin surfaces that are either untreated or treated with MPS5, MPS10, or MPS15. The water contact angles for the MPS5, MPS10, and MPS15 groups are higher than that for the untreated dentin surface ($P < 0.001$). There is no significant difference between the MPS5, MPS10, and MPS15 groups ($P = 0.142$, 0.054, and 0.957).

2.5. Microtensile Bond Strength (μTBS) Tests. The μTBS results (mean ± SD) are presented in Figure 3. Aging and primer-solution type both have a significant influence on μTBS ($P < 0.001$), but the interactions between them are not significant ($P = 0.982$). Statistical analysis results for the μTBS data are shown in Tables S2 and S3 (details given in the Supporting Information).

After 24 h water storage, the μTBS is the lowest for the control (CTR) group. The initial μTBS values for the MPS-alone groups are not significantly different to that for the CTR group ($P > 0.05$). However, the MDP-containing primer solutions all improve the initial μTBS value compared with the CTR group. The copresence of MPS at any concentration does not decrease the μTBS value compared with that of the MDP group ($P > 0.05$).

12 month water storage decreases μTBS for all the groups ($P < 0.05$). The μTBS values for the specimens conditioned with MDP-containing primer solutions (MDP, MPS5 + MDP, MPS10 + MDP, and MPS15 + MDP) are significantly higher than those treated with MPS or not, both before and after aging ($P < 0.05$). Furthermore, the MPS10 + MDP and MPS15 + MDP groups show a more severe decrease than the MDP groups ($P < 0.05$).

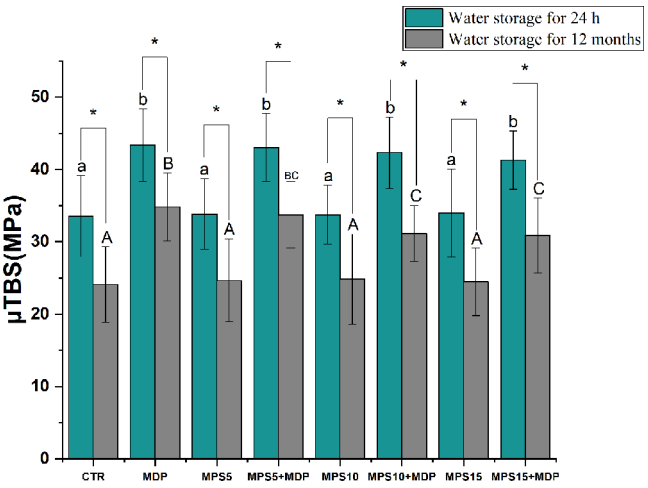

Figure 3. Means and standard deviations of μTBS values. Mean values are represented using different superscript lowercase letters (24 h water storage) and uppercase letters (12 month water storage) and showed significant differences ($P < 0.05$), *μTBS values were significantly different between 24 h water storage and 12 month water storage ($P < 0.05$).

2.6. Nanoleakage. As shown in Figure 4A−H, the CTR group shows extensive reticular-mode silver nitrate uptake at 24 h water storage. Additionally, the MPS5, MPS10, and MPS15 groups show a similar silver-ion-distribution pattern to that for the CTR group. Conversely, groups treated with MDP-containing primer show less silver nitrate deposition.

After 12 month water storage (Figure 4I−P), all the groups show much more serious nanoleakage. The CTR group exhibits the most severe nanoleakage after aging. Similar nanoleakage patterns are observed along the entire interface for the aged specimens, regardless of the application of MPS.

The MDP group exhibits the least silver nitrate leakage both after 24 h and 12 month water storage. The copresence of 10 or 15 wt % MPS results in a visible increase in silver deposits along the interface after aging compared with the MDP group.

2.7. In Situ Zymography. Activated matrix metalloproteinases (MMPs) hydrolyze fluorescein-quenched gelatin within the hybrid layer and dentinal tubules, resulting in green fluorescence. As shown in Figure 5, the hybrid layer and the dentine tubules in the CTR group present obvious green fluorescence similar to that for the MPS groups. The MDP-alone group shows much lower gelatinolytic activity, indicating that MMP activity is inhibited. However, when 10 or 15 wt % MPS is copresent with MDP, the green fluorescence intensity is increased.

3. DISCUSSION

We previously thought that silane can integrate collagen and resin by combining with the collagen network and enhancing its connection to resin.[11,13,14] However, we observed the opposite results in the present infrared, ultraviolet, and Raman spectra of MPS, wherein no new chemical bonds were introduced into the silane-treated collagen except for the Si−C and Si−O bonds from silane, and its structure remained unchanged, indicating that there was no chemical bonding between the MPS and dentin collagen, only weaker interaction. This is a new discovery

https://doi.org/10.1021/acsomega.2c01000
ACS Omega 2022, 7, 15892−15900

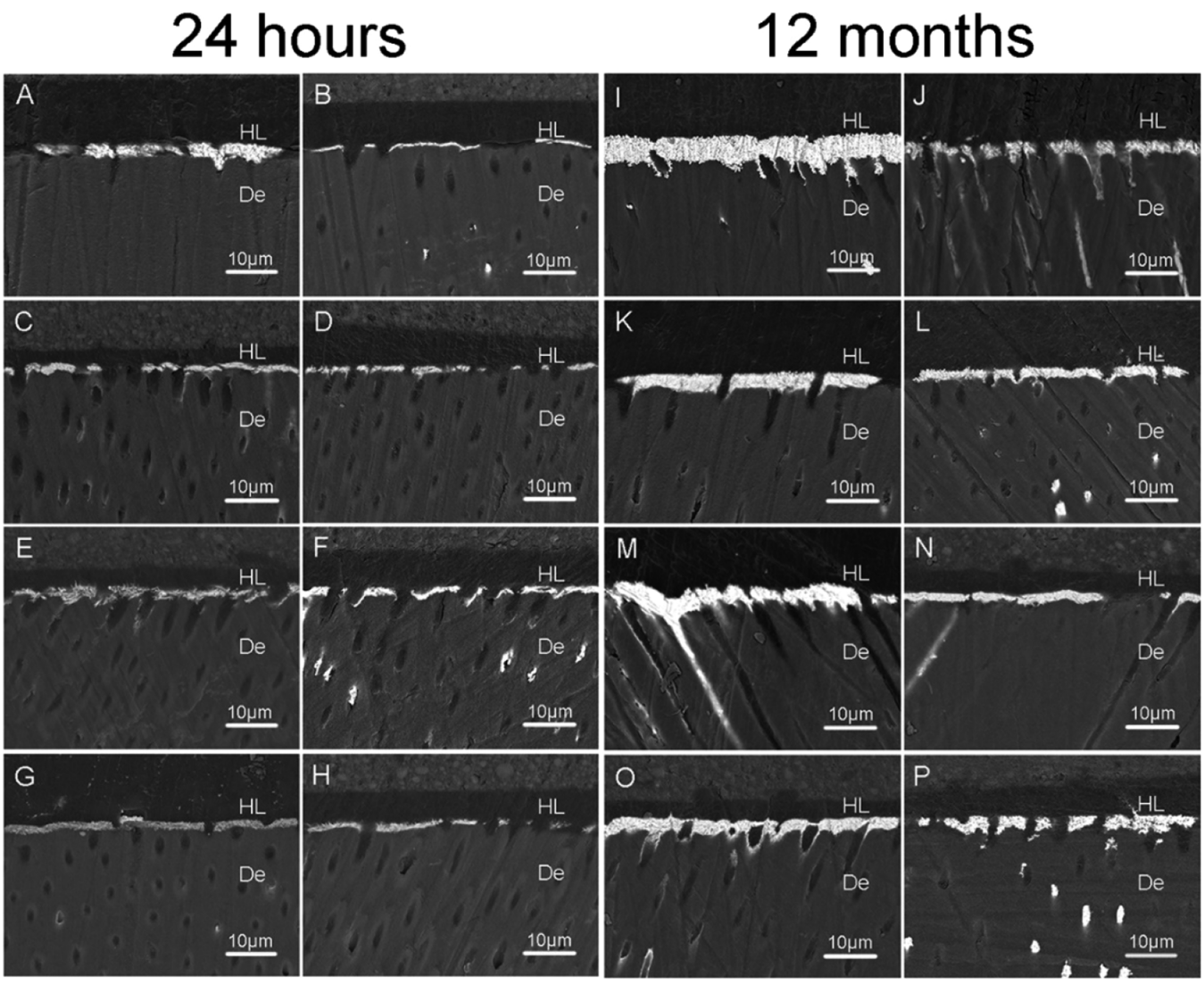

Figure 4. SEM images of resin−dentin interfaces for CTR (A,I), MDP (B,J), MPS5 (C,K), MPS5 + MDP (D,L), MPS10 (E,M), MPS10 + MDP (F,N), MPS15 (G,O), and MPS15 + MDP (H,P), showing the different silver deposition patterns after 24 h (A−H) and 12 month (I−P) water storage. HL: hybrid layer; De: dentin.

in terms of the role of silane in dentin-bonding interfaces. Thus, based on the current results, hypothesis (i) must be rejected.

Under ideal conditions, silane hydrolysates show weak interactions with collagen and adsorb on the collagen surface via van der Waals forces and hydrogen bonds. Regardless of the mode of type-I collagen, the more silanol groups in the hydrolysate, the stronger the hydrogen bonding it forms. Hence, the interaction mainly depends on the number of silanol groups produced by MPS hydrolysis.[29] This finding is consistent with the current chemical characterization results. This weak interaction is unstable and is of limited use for practical application. Only a small amount of Si was present on the collagen surface, suggesting that the unstable interaction between silane and collagen could be easily disrupted by even slight external forces, such as those encountered in washing. In addition, the current adhesives contain small amounts of silane, and the shelf life of silane may be shorter under acidic conditions. Silane loses its activity over time as it self-condenses to form Si−O−Si oligomers and fails to interact with collagen. The present μTBS test results further support the above findings. No significant difference is observed between the CTR group and MPS-treated groups after 24 h or 12 months of water storage, and the bonding strength is not improved ($P > 0.05$).

Although the interaction force between MPS and dentin is weak, in this study, the zeta potential of collagen silanized at different concentrations of MPS was significantly reduced compared with that of pure collagen to −23 mV. Zeta potential is one of the factors determining particle non-aggregation.[30] Collagen powders appear more stable regardless of the concentration of silane. At the same time, the surface of silanized dentin showed better hydrophobicity, which was also independent of silane concentration. The application of silane may therefore provide some degree of gain in collagen stability and hydrophobicity. Thus, the second hypothesis that "MPS influences the surface properties of collagen" has to be accepted. However, the benefits to dentine bonding performance are not clear.

Compared with the limited benefit of MPS, the adverse effect of the interaction between MPS and MDP on the bonded interface should be considered. Previous studies have confirmed that MDP and dentine hydroxyapatite can form water-insoluble MDP-calcium salts along the bonded interface[18,31,32] that

https://doi.org/10.1021/acsomega.2c01000
ACS Omega 2022, 7, 15892−15900

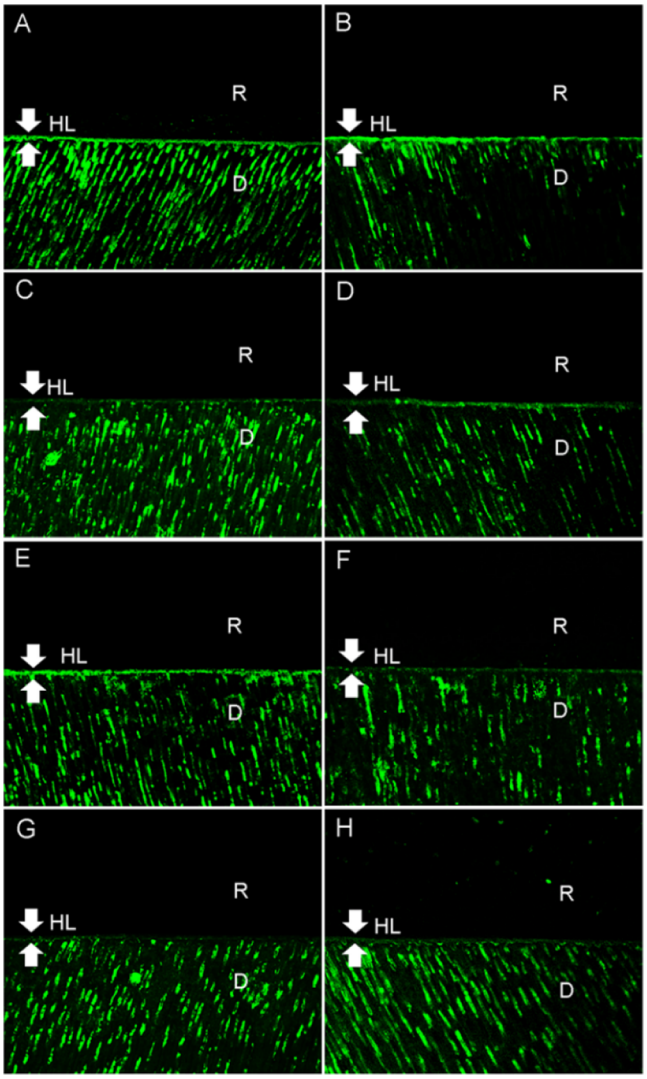

Figure 5. Representative images of the quenched fluorescein-conjugated gelatin substrate after 24 h incubation for CTR (A), MDP (B), MPS5 (C), MPS5 + MDP (D), MPS10 (E), MPS10 + MDP (F), MPS15 (G), and MPS15 + MDP (H), revealing green fluorescence in the dentinal tubules along the hybrid layer.

improve the dentin bonding strength and durability.[19,33] In the present study, the bonding strengths of the groups conditioned with the MDP-containing primer obtained at 24 h and 12 months are much higher than that of the CTR group. Furthermore, the μTBS values of all groups decreased after 12 month water storage. This can be explained by the mixing of high concentrations of MPS, which reduces the dentin bond strength significantly. After water storage, the adverse effect of MPS on the bonding performance is amplified. We speculate that the condensation reaction between copresent MPS and MDP in the primer consumes active MDP molecules that have chemical affinity with dentin. In addition, MPS continuously forms inactive macromolecules deposited on the dentine surface,[1] which occupy the contact area between MDP and hydroxyapatite, thus impeding their chemical binding potential. This phenomenon is also confirmed by the current nanoleakage and in situ zymography results. Thus, the third hypothesis that "the coexistence of MPS and MDP interferes with their beneficial effects on resin−dentin bonding" has to be accepted.

The exposed collagen fibers located at the bottom of the hybrid layer are surrounded by residual water, becoming a target of MMPs owing to the lack of protection by resin monomers.[34] Although MPS is adsorbed on the surface of dentin collagen and improves the hydrophobicity of the collagen surface, due to the strong hydrophilic nature of collagen itself, MPS is unable to make the collagen surface more hydrophobic. Therefore, collagen fibers still exist in a water-filled environment and thus still at risk of being hydrolyzed. According to the current in situ zymography results, the green fluorescence is similar to that of the CTR group when MPS is applied to the dentin-bonded interface, indicating that MPS conditioning plays a negligible role in inhibiting collagen degradation. The green fluorescence for the MDP group is more intermittently distributed than that for the CTR group, suggesting that MDP or MDP-calcium salts inhibit the activation of MMPs.[35] However, along with an increase in the amount of MPS, the level of green fluorescence increases, suggesting that the copresence of MPS prevents MMP inhibition by MDP or MDP-calcium salts.

Enhanced MMP activity indicates increased enzymatic hydrolysis of unprotected collagen fibers, degrading the integrity of the hybrid layer and thus resulting in increased nanoleakage. Therefore, the presence of MPS at high concentration causes more nanoleakage and a more significant decrease in μTBS after 12 month water storage. Although a high concentration of MPS prevents the inhibition of MMPs, there is no detectable change in initial μTBS because the degradation of the collagen fibers in the hybrid layer is time-dependent. Nanoleakage evaluated at 24 h showed that the silver nitrate distribution does not change significantly when different concentrations of MPS are present in the MDP-containing primer. The location of silver-ion deposition is filled with water, collagen fibers in these weak areas are hydrolyzed, and the adhesive resin monomer leaches out of the resin−dentin interface during water storage, thus degrading the integrality of the hybrid layer.[8] The silver ions are continuously arranged along the hybrid and adhesive layers after 12 month water storage. Compared to the MDP group, more silver deposits are observed when conditioned with different concentrations of MPS or not. Clearly, this is because the effect of MDP on improving dentin bonding performance is interfered with by MPS, leading to more serious nanoleakage and decreased μTBS. Therefore, although the single-step and single-bottle operation of the universal adhesive make it more user-friendly and convenient, it sacrifices some of the effect that each functional component achieves such as silane or MDP when used alone. Clinically, this may manifest as a decrease in the dentin-bonding performance. Thus, innovative research into one-bottle dental technologies that better preserve the full activity of each functional component is required.

4. CONCLUSIONS

Within the limitations of this in vitro study, the following conclusions were drawn: MPS adsorbs loosely on the dentin collagen surface through hydrogen bonding and van der Waals forces, slightly enhancing the hydrophobicity and zeta potential of the dentin surface. Silane applied alone neither significantly promotes the bonding nor has adverse effects on the bonded interface. However, the coexistence of MPS and MDP impairs their effectiveness and makes the resultant dentin bonding unstable. The coexistence of MPS and MDP in one bottle aggravates enzyme activity at the bonded interface compared to MDP alone, which intensifies the long-term nanoleakage of the bonded interface and reduces the bond durability.

https://doi.org/10.1021/acsomega.2c01000
ACS Omega 2022, 7, 15892−15900

The compositions are relative to the weight of the entire primer.

5. MATERIALS AND METHODS

5.1. Preparation of Primer Solutions. Experimental primers were prepared by mixing MPS (Macklin, Shanghai, China), MDP (DM Healthcare Products, Inc., San Diego, CA, USA), deionized water, and ethanol in different proportions in one bottle. Eight different experimental primers were prepared according to MDP and MPS contents. Table 1 lists the compositions and contents of the experimental primers.

Table 1. Compositions (wt %) of the Primer Solutions Used in This Study

group	MDP	MPS	deionized water	ethanol	pH
CTR	0	0	0	0	
MDP	10	0	15	75	2.68
MPS5	0	5	15	80	6.96
MPS5 + MDP	10	5	15	70	2.69
MPS10	0	10	15	75	7.11
MPS10 + MDP	10	10	15	65	2.63
MPS15	0	15	15	70	7.23
MPS15 + MDP	10	15	15	60	2.64

5.2. Interactions between Collagen and MPS. Collagen powder (C9879, Sigma Chemical Co., St. Louis, MO, USA) was dispersed in MPS5, MPS10, or MPS15 primer, rinsed with ethanol three times, and dried at room temperature. Untreated collagen powders were set as the control.

XPS (Escalab 250xi, Thermo Fisher Scientific, UK) using monochromatic A1Kα radiation (photoenergy = 1486.6 eV; energy step size = 0.05 eV) was carried out to study the MPS-conditioned collagen surfaces. Narrow-scan spectra of the Si 2p region were fitted using the XPS Peak 4.1 software.

Successful conditioning of the collagen powder with MPS was verified by FTIR spectroscopy (Nicolet 6700, Thermo Scientific, USA) in the transmission mode from 3500 to 500 cm^{-1} using the KBr pellet method.

A UV-3600 spectrophotometer (Shimadzu Corporation, Kyoto, Japan) was used to obtain the UV−vis spectra of collagen before and after treatment. The spectral range was 200−800 nm, and the scanning speed was 1 nm s^{-1}.

Raman spectroscopy (System-2000, Renishaw, UK) was used to characterize chemical changes associated with the adsorption of silane. Samples were analyzed using a 785 nm laser (<500 μW power) under a 100× objective lens. Spectra were collected in the range 400−3000 cm^{-1} with an accumulation time of 100 s.

5.3. Molecular Docking Simulations. In this study, because silanols with different numbers of Si−OH groups will be formed upon silane hydrolysis, we modeled four different hydrolysis configurations, termed MPS, MPS1, MPS2, and MPS3 (Figure 2). Three type-I collagen crystal structures with different amino acid residues were obtained from the Protein Data Bank. The amino acid sequences of the three forms are the following: 1CGD, $(Pro-Hyp-Gly)_4-(Pro-Hyp-Ala)-(Pro-Hyp-Gly)_5$;[36] 4OY5, $(Gly-Pro-Hyp)_{10}$;[37] and 1QSU, $(Pro-Gly-Hyp)_4-(Glu-Lys-Gly)-(Pro-Hyp-Gly)_5$.[38]

Using AutoDock docking software,[39] the ligand was set as a flexible molecule. Type-I collagen was confined to the grid box as a rigid static entity. Lamarckian genetic methods were used to explore all the possible conformations of the ligand that could bind to the target. The initial population of the Lamarckian genetic algorithm was 150 individuals, the maximum energy number evaluated was 2.5×10^6, and the maximum energy generated was 2.7×10^4. The value of the free binding energy of the complex was calculated using a semiempirical free capacity field.[40] The open-source software PyMOL (PyMOL Molecular Graphics System, version 0.99 Schrödinger, LLC.) was used to visualize the binding of the collagen−ligand complex.

5.4. Zeta Potential Measurement. Dry collagen powder (10 mg) was suspended in 1 mL deionized water. The sample was made into a homogeneous suspension by sonication. Zeta potential measurement was then performed using a Zetasizer Nano ZS (Malvern, UK).

5.5. Preparation of Dentin and Dentin-/Resin-Bonded Specimens. One hundred freshly extracted non-carious human third molars were used for in vitro research based on a protocol approved by the Ethics Committee of Nanjing Medical University, China [file number (2019)277]. The dentin specimens were prepared using a low-speed diamond saw (Isomet 1000, Buehler Ltd., Lake Bluff, IL, USA) and stored in Hank's balanced salt solution before analysis.

The surface was ground with a 600 grit SiC abrasive paper for 60 s and then etched using 35% phosphoric acid (Gluma Etch 35 Gel) for 15 s. After rinsing, excess moisture was removed using an absorbent paper. After treatment with the experimental primer solution, the surface was coated with a commercial adhesive (Single Bond 2, 3M ESPE, St. Paul, MN, USA). The composition and application procedures are listed in Table 2.

The other dentin slabs used for contact angle measurement were demineralized with 10% phosphoric acid (695017, Sigma Chemical Co., St. Louis, MO, USA) for 5 h and then irrigated with deionized water. After checking the demineralized dentine surface by digital radiography, the dentin surfaces were treated with the MPS5, MPS10, or MPS15 primer and air-dried for 20 s.

5.6. Contact Angle Measurement. Static contact angles were measured (Zhongchen Digital Technology Apparatus Co., Shanghai, China) using a 5 μL water droplet at room temperature. For all measurements, the distance from the tip to the surface was constant. A digital camera was used to capture droplet images. The contact angles were determined using ContactAngle software (Zhongchen Digital Technology Apparatus Co).

5.7. μTBS Tests. A 2 mm layer of resin composite (Filtek Z250, 3M ESPE) was placed on the bonded surface and cured

Table 2. Composition and Application Procedure of Single Bond 2

adhesive (manufacturer)	chemical formulation	application procedure
single bond 2 (3M/ESPE, St. Paul, MN, USA)	HEMA, bis-GMA, ethyl alcohol, silane-treated silica (nanofiller), glycerol 1,3-dimethacrylate, copolymer of acrylic and itaconic acids, diurethane dimethacrylate, and water	1. Acid etch for 15 s 2. Rinse for 15 s 3. Apply 2 consecutive coats 4. Gently air dry for 5 s 5. Light cure for 10 s

https://doi.org/10.1021/acsomega.2c01000
ACS Omega 2022, 7, 15892−15900

for 40 s twice. After storing in 37 °C distilled water for 24 h or 12 months, the bonded specimens were perpendicularly sectioned into 1 mm × 1 mm sticks. Each stick was subjected to μTBS testing using a universal testing machine (Instron 3365 ElectroPuls, Instron, USA). The loading speed was set at 1.0 mm/min, and the maximum load (N) at fracture was recorded. The μTBS was calculated based on the formula: μTBS (MPa) = maximum load (N)/bonded area (mm^2).

5.8. In Situ Zymography. A flowable resin composite (Filtek 350XT Flow; 3M ESPE) was applied to 1 mm thick mid-dentin. The bonding process was the same as in that used in the μTBS tests. The dentin−resin interface was exposed using a low-speed diamond saw (Isomet 1000, Buehler Ltd., Lake Bluff, IL, USA). The specimens were adhered to light microscope slides and ground to a thickness of 500 μm.[41] Self-quenched fluorescein-conjugated gelatin was employed as the matrix metalloproteinase (MMP) substrate (E-12055; Molecular Probes, Eugene, OR, USA).[42] After 24 h of incubation, hydrolysis of the quenched fluorescein-conjugated gelatin substrate, indicative of endogenous gelatinolytic enzyme activity, was assessed using confocal laser scanning microscopy (Zeiss LSM880 with NLO & Airyscan, Germany).

5.9. Nanoleakage. After immersion in water for 24 h or 12 months, eight μTBS sticks were cleaned ultrasonically, dried, and evenly applied with two layers of nail polish less than 1 mm from the bonding interface on both sides. Then, they were immersed in 50 wt % ammoniacal silver nitrate solution, shielded from light for 24 h,[43] and rinsed with running water. To reduce the penetrated silver ions into metallic silver grains, the specimens were soaked in a photograph development solution under fluorescent light for 8 h. The nanoleakage pattern was observed using a scanning electron microscope in the back-scattered electron mode (TESCAN MAIA3, Kohoutovice, Czech Republic).

5.10. Statistical Analysis. Histograms of contact angle and zeta potential data were drawn with GraphPad Prism (v.8.0.2.263) (GraphPad software, Inc., La Jolla, USA) and analyzed by one-way analysis of variance (ANOVA) with the Tukey−Kramer postdeviation test. The effects of primer solution and aging factors on μTBS were analyzed by two-way ANOVA with SPSS 21.0. Multicomparison analysis was performed using Tukey's post hoc least significant difference test. Significance was assumed at $P < 0.05$.

■ ASSOCIATED CONTENT

Supporting Information

The Supporting Information is available free of charge at https://pubs.acs.org/doi/10.1021/acsomega.2c01000.

Zeta potentials, water contact angles, and statistical analysis of μTBS data (PDF)

■ AUTHOR INFORMATION

Corresponding Author

Chen Chen − *Department of Endodontics, The Affiliated Stomatological Hospital of Nanjing Medical University, Jiangsu Province Key Laboratory of Oral Diseases, Jiangsu Province Engineering Research Center of Stomatological Translational Medicine, Nanjing 210029, China;* orcid.org/0000-0002-2989-180X; Email: ccchicy@njmu.edu.cn

Authors

Xin Jin − *Department of Endodontics, The Affiliated Stomatological Hospital of Nanjing Medical University, Jiangsu Province Key Laboratory of Oral Diseases, Jiangsu Province Engineering Research Center of Stomatological Translational Medicine, Nanjing 210029, China*

Xiaojun Yuan − *Department of Endodontics, The Affiliated Stomatological Hospital of Nanjing Medical University, Jiangsu Province Key Laboratory of Oral Diseases, Jiangsu Province Engineering Research Center of Stomatological Translational Medicine, Nanjing 210029, China*

Kai Chen − *Collaborative Innovation Center of Atmospheric Environment and Equipment Technology; Jiangsu Key Laboratory of Atmospheric Environment Monitoring and Pollution Control; School of Environmental Science and Engineering, Nanjing University of Information Science & Technology, Nanjing 210029, China*

Haifeng Xie − *Department of Prosthodontics, The Affiliated Stomatological Hospital of Nanjing Medical University; Jiangsu Province Key Laboratory of Oral Diseases; Jiangsu Province Engineering Research Center of Stomatological Translational Medicine, Nanjing 210029, China;* orcid.org/0000-0003-2008-3846

Complete contact information is available at: https://pubs.acs.org/10.1021/acsomega.2c01000

Author Contributions

‖Xin Jin and Xiaojun Yuan contributed equally to this work.

Notes

The authors declare no competing financial interest.

■ ACKNOWLEDGMENTS

The authors thank Yan Fang (NIGPAS, China) for providing technical support in SEM observation. This work was supported by the National Natural Science Foundation of China [grant 81970927], the Natural Science Foundation of Jiangsu Province of China [BK20191348], and the Qing Lan Project and the Priority Academic Program Development of Jiangsu Higher Education Institutions [grant 2018-87].

■ REFERENCES

(1) Chen, B.; Lu, Z.; Meng, H.; Chen, Y.; Yang, L.; Zhang, H.; Xie, H.; Chen, C. Effectiveness of pre-silanization in improving bond performance of universal adhesives or self-adhesive resin cements to silica-based ceramics: Chemical and in vitro evidences. *Dent. Mater.* **2019**, *35*, 543−553.

(2) Matinlinna, J. P.; Lung, C. Y. K.; Tsoi, J. K. H. Silane adhesion mechanism in dental applications and surface treatments: A review. *Dent. Mater.* **2018**, *34*, 13−28.

(3) Filho, A. M.; Vieira, L. C. C.; Araújo, É.; Monteiro Júnior, S. Effect of different ceramic surface treatments on resin microtensile bond strength. *J. Prosthodont.* **2004**, *13*, 28−35.

(4) Shahverdi, S.; Canay, S.; Sûahin, E.; Bilge, A. Effects of different surface treatment methods on the bond strength of composite resin to porcelain. *J. Oral Rehabil.* **1998**, *25*, 699−705.

(5) Gidi, Y.; Bayram, S.; Ablenas, C. J.; Blum, A. S.; Cosa, G. Efficient One-Step PEG-Silane Passivation of Glass Surfaces for Single-Molecule Fluorescence Studies. *ACS Appl. Mater. Interfaces* **2018**, *10*, 39505−39511.

(6) Yoshihara, K.; Nagaoka, N.; Maruo, Y.; Nishigawa, G.; Yoshida, Y.; Van Meerbeek, B. Silane-coupling effect of a silane-containing self-adhesive composite cement. *Dent. Mater.* **2020**, *36*, 914−926.

(7) Aydınoğlu, A.; Yoruç, A. B. H. Effects of silane-modified fillers on properties of dental composite resin. *Mater. Sci. Eng., C* **2017**, *79*, 382−389.
(8) Breschi, L.; Maravic, T.; Cunha, S. R.; Comba, A.; Cadenaro, M.; Tjäderhane, L.; Pashley, D. H.; Tay, F. R.; Mazzoni, A. Dentin bonding systems: From dentin collagen structure to bond preservation and clinical applications. *Dent. Mater.* **2018**, *34*, 78−96.
(9) Fawzy, A. S. Variations in collagen fibrils network structure and surface dehydration of acid demineralized intertubular dentin: effect of dentin depth and air-exposure time. *Dent. Mater.* **2010**, *26*, 35−43.
(10) Yu, F.; Luo, M. L.; Xu, R. C.; Huang, L.; Zhou, W.; Li, J.; Tay, F. R.; Niu, L. N.; Chen, J. H. Evaluation of a Collagen-Reactive Monomer with Advanced Bonding Durability. *J. Dent. Res.* **2020**, *99*, 813−819.
(11) Raghavan, R. N.; Muthukumar, T.; Somanathan, N.; Sastry, T. P. Biomimetic mineralization of novel silane crosslinked collagen. *Mater. Sci. Eng., C* **2013**, *33*, 1983−1988.
(12) Marín-Pareja, N.; Salvagni, E.; Guillem-Marti, J.; Aparicio, C.; Ginebra, M. P. Collagen-functionalised titanium surfaces for biological sealing of dental implants: effect of immobilisation process on fibroblasts response. *Colloids Surf., B* **2014**, *122*, 601−610.
(13) Siddique, A.; Meckel, T.; Stark, R. W.; Narayan, S. Improved cell adhesion under shear stress in PDMS microfluidic devices. *Colloids Surf., B* **2017**, *150*, 456−464.
(14) Marín-Pareja, N.; Cantini, M.; González-García, C.; Salvagni, E.; Salmerón-Sánchez, M.; Ginebra, M. P. Different Organization of Type I Collagen Immobilized on Silanized and Nonsilanized Titanium Surfaces Affects Fibroblast Adhesion and Fibronectin Secretion. *ACS Appl. Mater. Interfaces* **2015**, *7*, 20667−20677.
(15) Chen, Y.; Wang, Y.; Feng, C.; He, Q.; Chen, Q.; Wang, Z.; Han, Q. Novel quat/di-N-halamines silane unit with enhanced synergism polymerized on cellulose for development of superior biocidability. *Int. J. Biol. Macromol.* **2020**, *154*, 173−181.
(16) Rosa, W. L. d. O. d.; Piva, E.; Silva, A. F. d. Bond strength of universal adhesives: A systematic review and meta-analysis. *J. Dent.* **2015**, *43*, 765−776.
(17) Yuan, X.; Wang, Q.; Han, F.; Chen, C.; Xie, H. Chemical interaction between 10-methacryloyloxydecyl dihydrogen phosphate and methacryloxypropyltrimethoxysilane in one-bottle dental primer and its effect on dentine bonding. *J. Mech. Behav. Biomed. Mater.* **2021**, *121*, 104610.
(18) Yoshihara, K.; Hayakawa, S.; Nagaoka, N.; Okihara, T.; Yoshida, Y.; Van Meerbeek, B. Etching Efficacy of Self-Etching Functional Monomers. *J. Dent. Res.* **2018**, *97*, 1010−1016.
(19) Yaguchi, T. Layering mechanism of MDP-Ca salt produced in demineralization of enamel and dentin apatite. *Dent. Mater.* **2017**, *33*, 23−32.
(20) Fehrenbach, J.; Isolan, C. P.; Münchow, E. A. Is the presence of 10-MDP associated to higher bonding performance for self-etching adhesive systems? A meta-analysis of in vitro studies. *Dent. Mater.* **2021**, *37*, 1463−1485.
(21) Nagaoka, N.; Yoshihara, K.; Feitosa, V. P.; Tamada, Y.; Irie, M.; Yoshida, Y.; Van Meerbeek, B.; Hayakawa, S. Chemical interaction mechanism of 10-MDP with zirconia. *Sci. Rep.* **2017**, *7*, 45563.
(22) Yoshihara, K.; Nagaoka, N.; Sonoda, A.; Maruo, Y.; Makita, Y.; Okihara, T.; Irie, M.; Yoshida, Y.; Van Meerbeek, B. Effectiveness and stability of silane coupling agent incorporated in 'universal' adhesives. *Dent. Mater.* **2016**, *32*, 1218−1225.
(23) Stani, C.; Vaccari, L.; Mitri, E.; Birarda, G. FTIR investigation of the secondary structure of type I collagen: New insight into the amide III band. *Spectrochim. Acta, Part A* **2020**, *229*, 118006.
(24) Ye, H.; Rahul; Kruger, U.; Kruger, U.; Wang, T.; Shi, S.; Norfleet, J.; De, S. Burn-related Collagen Conformational Changes in ex vivo Porcine Skin using Raman Spectroscopy. *Sci. Rep.* **2019**, *9*, 19138.
(25) Ju, H.; Liu, X.; Zhang, G.; Liu, D.; Yang, Y. Comparison of the Structural Characteristics of Native Collagen Fibrils Derived from Bovine Tendons using Two Different Methods: Modified Acid-Solubilized and Pepsin-Aided Extraction. *Materials* **2020**, *13*, 358.
(26) Khung, Y. L.; Ngalim, S. H.; Meda, L.; Narducci, D. Preferential formation of Si-O-C over Si-C linkage upon thermal grafting on hydrogen-terminated silicon (111). *Chemistry* **2014**, *20*, 15151−15158.
(27) Costa, B. M. F.; Freitas, D. V.; Sousa, F. L. N.; Silva, K. D.; Dias, J. M. M.; Assis, A. M. L.; Jesus, A. C.; Ribeiro, A. S.; Navarro, M. Sats@cdte hierarchical structures emitting green to red colors developed for latent fingerprint applications. *Dyes Pigm.* **2020**, *180*, 108483.
(28) Cardenas, A. M.; Siqueira, F.; Hass, V.; Malaquias, P.; Gutierrez, M. F.; Reis, A.; Perdigão, J.; Loguercio, A. Effect of MDP-containing Silane and Adhesive Used Alone or in Combination on the Long-term Bond Strength and Chemical Interaction with Lithium Disilicate Ceramics. *J. Adhes. Dent.* **2017**, *19*, 203−212.
(29) Bento, A. P.; Bickelhaupt, F. M. Nucleophilic substitution at silicon (SN2@Si) via a central reaction barrier. *J. Org. Chem.* **2007**, *72*, 2201−2207.
(30) Cardoso, R. F. d. M.; Basting, R. T.; França, F. M. G.; Amaral, F. L. B. d.; Basting, R. T. Physicochemical characterization, water sorption and solubility of adhesive systems incorporated with titanium tetrafluoride, and its influence on dentin permeability. *J. Mech. Behav. Biomed. Mater.* **2021**, *119*, 104453.
(31) Zhao, Q.; Han, F.; Yuan, X.; Chen, C. Effects of Solvents and pH Values on the Chemical Affinity of 10-Methacryloyloxydecyl Dihydrogen Phosphate toward Hydroxyapatite. *ACS Omega* **2021**, *6*, 19183−19193.
(32) Yoshihara, K.; Nagaoka, N.; Yoshida, Y.; Van Meerbeek, B.; Hayakawa, S. Atomic level observation and structural analysis of phosphoric-acid ester interaction at dentin. *Acta Biomater.* **2019**, *97*, 544−556.
(33) Tsujimoto, A.; Barkmeier, W. W.; Takamizawa, T.; Watanabe, H.; Johnson, W. W.; Latta, M. A.; Miyazaki, M. Comparison between universal adhesives and two-step self-etch adhesives in terms of dentin bond fatigue durability in self-etch mode. *Eur. J. Oral Sci.* **2017**, *125*, 215−222.
(34) Breschi, L.; Prati, C.; Gobbi, P.; Pashley, D.; Mazzotti, G.; Teti, G.; Perdigão, J. Immunohistochemical analysis of collagen fibrils within the hybrid layer: a FEISEM study. *Oper. Dent.* **2004**, *29*, 538−546.
(35) Shen, J.; Xie, H.; Wang, Q.; Wu, X.; Yang, J.; Chen, C. Evaluation of the interaction of chlorhexidine and MDP and its effects on the durability of dentin bonding. *Dent. Mater.* **2020**, *36*, 1624−1634.
(36) Kramer, R. Z.; Venugopal, M. G.; Bella, J.; Mayville, P.; Brodsky, B.; Berman, H. M. Staggered molecular packing in crystals of a collagen-like peptide with a single charged pair. *J. Mol. Biol.* **2000**, *301*, 1191−1205.
(37) Bella, J.; Brodsky, B.; Berman, H. M. Hydration structure of a collagen peptide. *Structure* **1995**, *3*, 893−906.
(38) Vaidyanathan, J.; Ravichandran, S.; Vaidyanathan, T.; Vaidyanathan, J.; Ravichandran, S.; Vaidyanathan, T. Computational analysis of adhesion of primer ligands to dentinal collagen: effect of spacer groups in ligand and amino Acid residue sequence differences in collagen. *Curr. Drug Discovery Technol.* **2007**, *4*, 150−161.
(39) Morris, G. M.; Huey, R.; Lindstrom, W.; Sanner, M. F.; Belew, R. K.; Goodsell, D. S.; Olson, A. J. AutoDock4 and AutoDockTools4: Automated docking with selective receptor flexibility. *J. Comput. Chem.* **2009**, *30*, 2785−2791.
(40) Vaidyanathan, J.; Vaidyanathan, T. K.; Kerrigan, J. E. Evaluation of intermolecular interactions of self-etch dentin adhesive primer molecules with type 1 collagen: computer modeling and in vitro binding analysis. *Acta Biomater.* **2007**, *3*, 705−714.
(41) Mancuso, E.; Comba, A.; Mazzitelli, C.; Maravic, T.; Josic, U.; Del Bianco, F.; Tay, F. R.; Breschi, L.; Mazzoni, A. Bonding to dentin using an experimental zirconium oxynitrate etchant. *J. Dent.* **2021**, *108*, 103641.
(42) Mazzoni, A.; Apolonio, F. M.; Saboia, V. P. A.; Santi, S.; Angeloni, V.; Checchi, V.; Curci, R.; Di Lenarda, R.; Tay, F. R.; Pashley, D. H.; et al. Carbodiimide inactivation of MMPs and effect on dentin bonding. *J. Dent. Res.* **2014**, *93*, 263−268.
(43) Tay, F. R.; Pashley, D. H.; Yoshiyama, M. Two modes of nanoleakage expression in single-step adhesives. *J. Dent. Res.* **2002**, *81*, 472−476.

https://doi.org/10.1021/acsomega.2c01000
ACS Omega 2022, 7, 15892−15900